

This work is licensed under the Creative Commons Attribution-NonCommercial-NoDerivatives 4.0 License (<https://creativecommons.org/licenses/by-nc-nd/4.0/>).

et al. 2008). Conidiation includes a period of vegetative growth (Bosch and Yantorno 1999) and is involved in conidial germination, mycelium formation, thick-walled foot cell formation at the tip of the aerial mycelium, and the production of multinuclear conidiophores.

In contrast with aerial conidia (CO), blastospores (BS) are produced by hyphal constriction, separation at the septa, and yeast-like budding. In insect mycology, BS are commonly referred to as any hyphal bodies produced in insect blood by hyphal budding, so BS are also considered hyphal bodies (Fargues et al. 2002). CO and BS are two different sporulation patterns that occur in the life cycle of *M. acridum*, and they are significantly different in cell morphology, structure, and activity. Conidiation is of crucial importance because conidia are infectious propagules and active components in mycoinsecticides. However, the high production cost and poor conidia production efficacy have retarded their application as mycoinsecticides (Lacey et al. 2001; Hajek et al. 2007). Thus, the BS were studied because of the lower cost of using industrial fermenting tanks (Adámek 1963). However, their thinner cell walls and lower tolerance to environmental stress and storage stability limit their application in the field (Pereira and Roberts 1990). Although BS have several drawbacks, they have other advantages, such as a fast germination rate and higher spore activity and virulence, so BS are usually used for seeds in solid-state fermentation (Hegedus et al. 1992; Faria and Wraight 2007). Most previous studies on the difference between CO and BS have focused on visual characteristics, virulence, storage conditions, and field application (Hegedus et al. 1992; Stephan et al. 1997; Leland et al. 2005; Wassermann et al. 2016). Nevertheless, little is known about the difference between the morphologies of CO and BS in entomopathogenic fungi on the transcriptome levels.

MicroRNAs (miRNAs) are a class of small non-coding RNA molecules that are approximately 22 nucleotides (nt) in length, which can partially or entirely bind to the 5'-UTR, 3'-UTR, or coding region of target genes to down- or up-regulate the expression of target genes (Grey et al. 2010; Fang and Rajewsky 2011; Reczko et al. 2012; Helwak et al. 2013; Hussain et al. 2013; Asgari 2014). These miRNAs are pervasive in animals and plants and act as posttranscriptional regulators that specifically guide target gene recognition to regulate gene transcriptional start or repression (Carthew and Sontheimer 2009). In animals, miRNAs have been shown to play important roles in cell development, proliferation, and differentiation. Targeted silencing of miRNA-132-3p expression is an advantage for bone marrow-derived mesenchymal stem cells (BMSC) osteogenic differentiation and osteogenesis (Hu et al. 2020). The overexpression of miRNA-324-5p exerts cell growth and migration-promoting effects through

activating Wnt signaling pathway and epithelial to mesenchymal transition (EMT) by negatively regulatory *suppressor of fused* gene (*SUFU*) in gastric carcinomas (Peng et al. 2020). Chi-miR-199a-5p inhibited *TGF- β 2* expression at both mRNA and protein translation levels in fibroblasts (Han et al. 2020). In plants, they also play various roles in plant development, stress response, and antibacterial resistance. MiRNA157 regulated floral organ growth and ovule production in *Gossypium hirsutum* by negatively regulatory *promoter-binding protein-like* (*SPL*) gene (Liu et al. 2017), and miRNA156 could increase tolerance to heat stress by downregulating *promoter-binding protein-like* (*SPL*) gene in *Arabidopsis* (Stief et al. 2014). In fungi, miRNA-like RNAs (milRNAs), with similar characteristics to miRNAs in animals and plants, were discovered in *Neurospora crassa*. They are produced by at least four diverse pathways that use a distinct combination of factors, including QDE-2, Dicers, the exonuclease QIP, and an RNase III domain-containing protein, MRPL3 (Lee et al. 2010). Subsequently, milRNAs in various species of fungi were discovered, such as *Cordyceps militaris*, *Metarhizium anisopliae*, *Magnaporthe oryzae*, *Aspergillus fumigatus*, *Aspergillus flavus*, and *Penicillium marneffei* (Zhou et al. 2012; Lau et al. 2013; Özkan et al. 2017; Li et al. 2020).

In recent years, many studies have reported that milRNAs can affect the diverse physiological process in organisms, such as cell growth, development, virulence, metamorphosis, and metabolism (Mukherjee and Vilcinskis 2014; Ylla et al. 2017; Zhang et al. 2018; Guo et al. 2020). In *P. marneffei*, milRNAs regulated the growth process of mycelial and yeast phases (Lau et al. 2013). Ssc-milR-240 was shown to potentially regulate sclerotial development by epigenetic regulation of its target histone acetyltransferase in *Sclerotinia sclerotiorum* (Xia et al. 2020). Overexpression of milRNA-87 exhibited a dramatic increase in the growth, conidiation, and virulence of *Fusarium oxysporum* f. sp. *cubense* by silencing target gene (glycosyl hydrolase coding gene, *FOIG_15013*) expression (Li et al. 2022). In *Verticillium dahlia*, milRNA-1 regulated the virulence by binding to the 3'-UTR of a hypothetical protein-coding gene (*VdHy1*) for transcriptional repression (Jin et al. 2019). In *Fusarium graminearum*, milRNA-2 combined with 3'-UTR of *bioH1* involved in biotin biosynthesis to regulate biotin synthesis (Guo et al. 2019). MilR236 was shown to regulate appressorium formation and virulence of *M. oryzae* by binding to *MoHat1*, a histone acetyltransferase type B catalytic subunit (Li et al. 2020), and miR4 and miR16, which are involved in mycelium growth and sexual development in *C. militaris* (Shao et al. 2019). Hence, milRNAs may play an important role in *M. acridum*. The study of milRNAs and the expression profiles may help us better understand the roles in spore morphological differences in *M. acridum*.

M. acridum is an unusually effective model for studying spore morphological differentiation. Previous research has mainly focused on the cell structure and application of CO and BS in filamentous fungi. Nevertheless, very little information is known about the roles of milRNAs in spore morphological differences. Thus, in the present study, the cDNA and small RNA libraries from CO and BS of *M. acridum* were sequenced, and the DEMs and DEGs between CO and BS samples were screened to elucidate the biological function of milRNAs in spore morphological differences in *M. acridum*. Our study aimed to provide primary data for further research on spore morphological differences in *M. acridum*.

Experimental

Materials and Methods

Preparation of *M. acridum* samples. Wild-type (WT) *M. acridum* was obtained from the China General Microbiological Culture Collection Center (CGMCC, No. 0877). WT strains were grown on ¼ SDAY liquid and solid medium (1% dextrose, 0.25% peptone, 0.5% yeast extract, and 2% agar, w/v) at 28°C for 3 d to obtain blastospores (BS) and conidia (CO), respectively. The spores were harvested at 3 d in ddH₂O, and the resulting spore suspension was filtered with four layers of lens tissue to remove mycelia and medium. After collection, pure BS and CO were immediately used for RNA extraction.

RNA extraction and library sequencing. Total RNA was extracted from BS and CO using TRIzol reagent (Invitrogen, USA). The quality and concentration of the extracted RNAs were assessed by a Nanodrop ND-2000 spectrophotometer (Thermo Scientific, USA) and 2% agarose gel electrophoresis. According to the manufacturer's instructions, the mRNA libraries were constructed using TruSeq Stranded Total RNA Library Prep Kit with Ribo-Zero Gold for Illumina (NEB, USA). Briefly, the first-strand cDNA was synthesized using a random hexamer primer, which was followed by the synthesis of the second-strand cDNA. After 3' ends were adenylated, the cDNA was ligated to adaptors, followed by enriched DNA fragments. The length and quality of libraries were validated by Agilent Technologies 2100 Bioanalyzer (Agilent Technologies, USA).

According to the manufacturer's instructions, small RNA libraries were constructed using TruSeq Small RNA Sample Prep Kits for Illumina. Briefly, the 3' and 5' adaptors were ligated to milRNA, which was followed by reverse transcription and amplification. Then, PCR amplification was performed, and PCR products were purified on an 8% polyacrylamide gel (148 V, 1 h). Bands of 147 nt and 157 nt lengths were recovered

with gel extraction. Finally, the quality of libraries was validated by Agilent Technologies 2100 Bioanalyzer (Agilent Technologies, USA). Small RNA and mRNA library sequencing and analysis were conducted by OE Biotech Co., Ltd., Shanghai, China.

Sequence analysis. To obtain high-quality reads, the adaptors were removed by Trimmomatic software, and the low-quality bases, N bases and low-quality reads were filtered out (Bolger et al. 2014). The clean reads were aligned to the *M. acridum* genome and assessed by genomic and gene alignment using hisat2 (Kim et al. 2015). The sequencing reads were mapped to mRNA transcript sequences; the quantitative gene analysis was performed, and FPKM (Fragments Per Kilobase of Exon Per Million Fragments Mapped) values and count values were obtained by eXpress.

For small RNA library data, raw data with a 5' adaptor and poly (A) were removed, and low-quality reads shorter than 15 nt and reads longer than 41 nt were filtered out from the raw data to obtain clean data. Then, the clean reads were mapped to the *M. acridum* genome to calculate the percentage of the genome and subjected to a BLAST search against Rfam v. 10.1 (<http://www.sanger.ac.uk/software/Rfam>) and GenBank databases (<http://www.ncbi.nlm.nih.gov/genbank>) to remove annotated rRNAs, tRNAs, small nuclear RNAs (snRNAs), and small nucleolar RNAs (snoRNAs). Degraded fragments of mRNA and repeat sequences were filtered out by RepeatMasker (<http://www.repeatmasker.org>). The conserved milRNAs were identified by aligning against miRbase v. 21 database (<http://www.mirbase.org>), and used mirdeep2 to predict the novel miRNAs, and based on the hairpin structure of a pre-milRNA and miRbase database to identify the corresponding milRNA sequence. The sequencing data obtained from this study were deposited in NCBI's Sequence Read Archive (SRA) database under the number SAMN17192759.

Differentially expressed genes (DEGs) and milRNA (DEMs) analysis. The transcription levels of the two groups were measured based on the number of clean reads aligned to the genome. The numbers of mapped clean reads were normalized to FPKMs (Fragments Per Kilobase of Exon Per Million Fragments Mapped) using Cuffdiff (v. 2.1.1) (Trapnell et al. 2012). DEGs analysis was performed by the DESeq (2012) R package. Transcripts with *p*-values ≤ 0.05 and a fold change (FC) ≥ 2 were identified as DEGs. The differential mRNA Gene Ontology (GO) and Kyoto Encyclopedia of Genes and Genomes (KEGG) enrichments were analyzed by the hypergeometric distribution test.

The expression levels of milRNAs were normalized using TPM (Transcripts Per Million) with the following criteria:

$$\text{normalized expression} = \frac{(\text{mapped milRNA reads})}{(\text{total clean reads} \times 10^6)}$$

DEMs analysis was performed by the DESeq (2012) R package. The significance threshold was set to p -values ≤ 0.05 and fold change (FC) ≥ 2 in this study.

Target prediction and functional analysis of milRNA. The targets of DEMs were predicted by using miRanda software (v. 3.3a) with the following parameters: $S \geq 150$, $\Delta G \leq -30$ kcal/mol, and demand strict 5' seed pairing (Tiño 2009), the rangefinder was used for milRNA target prediction (Fahlgren and Carrington 2010). The GO enrichment and KEGG pathway enrichment of differentially expressed target genes were performed using R based on the hypergeometric distribution.

Quantitative real-time PCR (qRT-PCR) validation. To validate the differential expression of mRNAs and milRNAs between BS and CO in *M. acridum*, the relative expression levels of mRNA and milRNA were analyzed by qRT-PCR. As described above, the total RNAs of BS and CO were extracted using TRIzol reagent (Invitrogen, USA). First-strand cDNA was synthesized as follows: a total of 1 μ g RNA was applied with an oligo-dT primer using PrimeScript™ RT Master Mix (TaKaRa, China). A total of 1 μ g milRNA was reverse transcribed with a TaqMan MicroRNA Reverse Transcription Kit using small RNA-specific and stem-loop RT primers (Applied Biosystems, USA). All qRT-PCRs of samples were performed in triplicate. The 5.8S rRNA and glyceraldehyde-3-phosphate dehydrogenase gene (gpd) were used as reference genes to normalize milRNA and mRNA levels, respectively. Primers are listed in Table SI.

Results

mRNA expression profiles. To explore the expression patterns and co-expression of differentially expressed genes (DEGs) in different spore types, i.e., conidia (CO) and blastospores (BS), cDNA libraries from BS and CO were sequenced. As shown in Table I, 567,108,002 reads were obtained from six cDNA libraries after filtering, including 287,099,910 and 280,008,092 from BS and CO, respectively. More than 94.06% of raw

reads had Q-phred scores at the Q30 level (an error threshold of less than 0.01%), the BS and CO reads had approximately 46.96% GC content, and more than 64.94% of clean reads were mapped to the genome.

Gene expression was normalized to FPKM (Fragments Per Kilobase of Exon Per Million Fragments Mapped) in the present study. A total of 9,692 expressed genes were found in BS and CO in *M. acridum*, and the gene expression distribution was obtained in different samples (Fig. 1A). A total of 4,646 DEGs were found between BS and CO, containing 2,640 upregulated and 2,006 downregulated genes, with the criteria as follows: p -values ≤ 0.05 and fold change (FC) ≥ 2 (Fig. 1B). A correlation analysis showed that *M. acridum* exhibited a significant difference between BS and CO, indicating that there was transcriptional strong differentiation between BS and CO (Fig. 1C).

Functional analysis of the differentially expressed genes (DEGs). To better reveal the function, roles, and biological processes of DEGs in different spore types, Gene Ontology (GO) and Kyoto Encyclopedia of Genes and Genomes (KEGG) pathway enrichment analyses were performed to evaluate the function of 4,646 DEGs using DAVID (the Database for Annotation, Visualization and Integrated Discovery, v. 6.8, <https://david.ncifcrf.gov>). GO enrichment analyses included categorization into the biological process (BP), cell component (CC) and molecular function (MF). A total of 2,951 DEGs were annotated in 54 GO classes at GO level 2 (Fig. 2A). For BP analyses, most genes were involved in biological (1,919), metabolic (1,750), and single-organism processes (1,494). When GO classification was based on CC, most genes were assigned to the cell (2,094), cell part (2,089), and organelle (1,596). Among the MFs, catalytic activity (1,805) was the most commonly represented, followed by binding (1,571).

According to KEGG enrichment analyses, a total of 1,076 DEGs were subdivided into 256 KEGG pathways (Table SII). The KEGG database classified these genes into 33 pathways at the second level of classification. Among which the most significantly enriched pathways were carbohydrate metabolism (193), amino acid metabolism (183), translation (171), and global

Table I
Summary of mRNA sequencing reads from BS and CO in *M. acridum*.

Treatment	Raw reads	Clean reads	Clean bases	Q30 (%)	GC (%)	Mapped reads
BS1	98,843,641	95,572,956	14.02G	94.06%	47.09%	67,073,032 (70.18%)
BS2	98,842,417	95,807,416	14.02G	94.30%	46.33%	63,815,312 (66.61%)
BS3	98,841,869	95,719,538	13.98G	94.28%	45.60%	62,158,068 (64.94%)
CO1	91,944,126	90,288,984	13.30G	95.74%	48.16%	68,087,397 (75.41%)
CO2	98,843,196	97,087,780	14.31G	95.79%	47.56%	71,191,515 (73.33%)
CO3	94,432,568	92,631,328	13.62G	95.68%	46.99%	666,88,341 (71.99%)

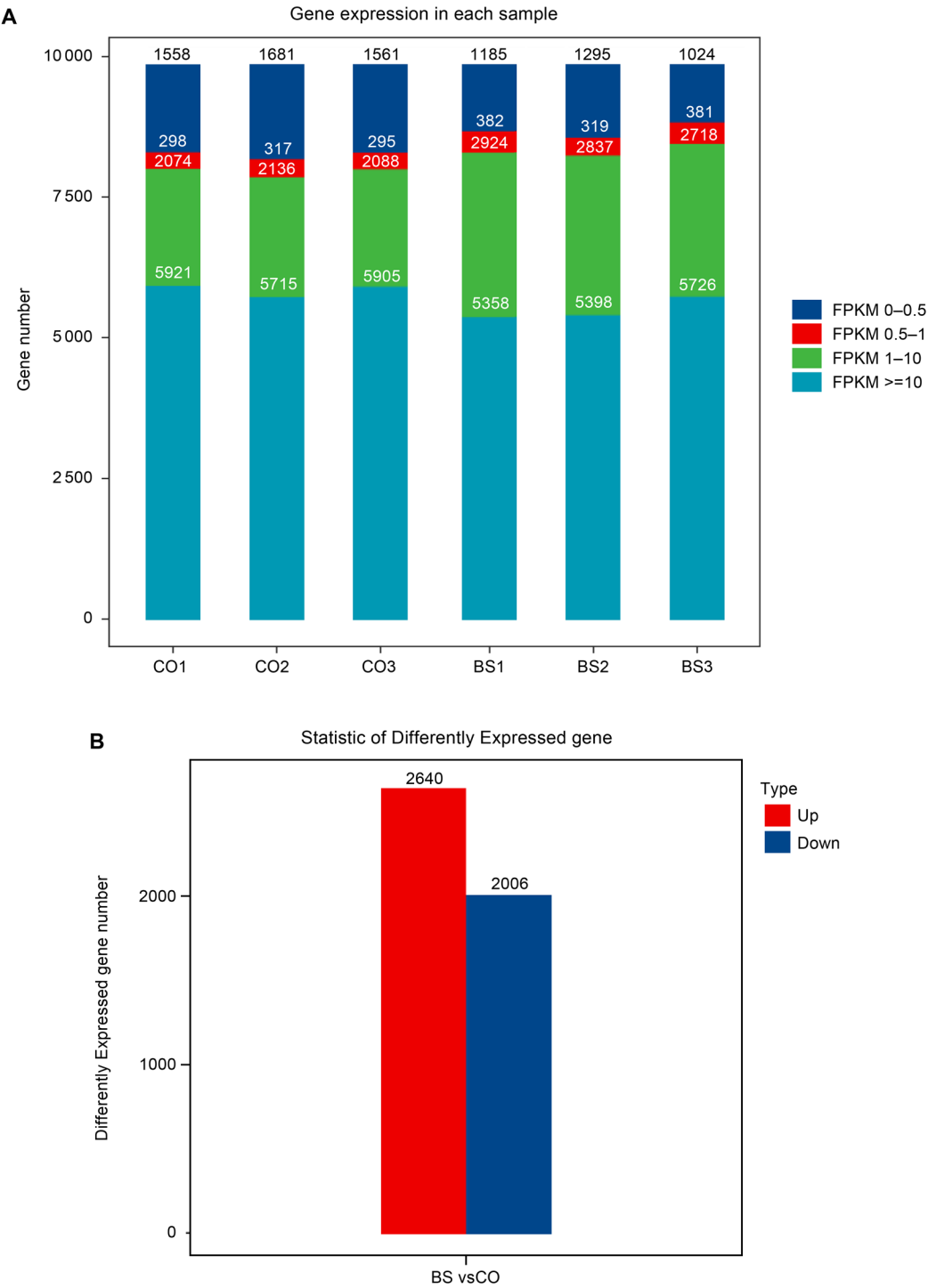


Fig. 1. Overview of mRNA expression profiles and DEGs in BS and CO.
A) The gene expression distribution. B) The DEGs in BS and CO, significantly downregulated genes, and upregulated genes are identified with $|\log_2 FC| \geq 1$ and p -values ≤ 0.05 .

and overview maps (164) (Fig. 2B). The top 20 of 33 significantly enriched pathways showed that the most significantly enriched pathways were biosynthesis of amino acids, carbohydrate metabolism, ribosome, and oxidative phosphorylation (Fig. 2C). These results suggested that the DEGs were mainly involved in metabolism of BS and CO, which might be associated with cell activity and structure.

Analysis of miRNA sequences. To explore the regulation of gene expression by miRNAs in different spore types, i.e., BS and CO, six small RNA libraries were sequenced. A total of 81,627,529 raw reads were generated from six small RNA libraries, and after filtering, 67,072,593 clean reads were obtained from BS and CO samples. Clean reads were aligned against the small RNA database and annotated, and an

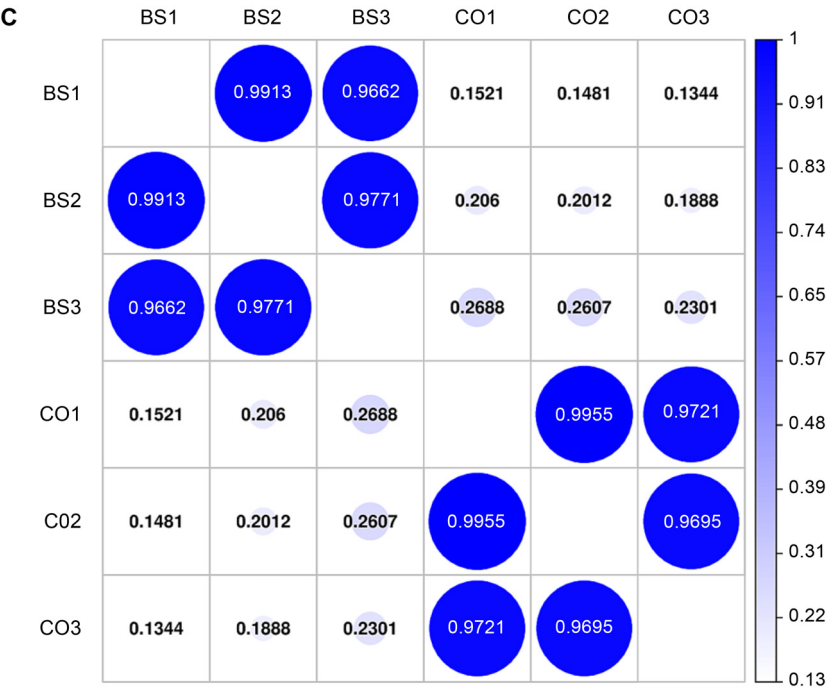


Fig. 1. Overview of mRNA expression profiles and DEGs in BS and CO.
C) Heatmap of Pearson correlations of the expression levels among samples.

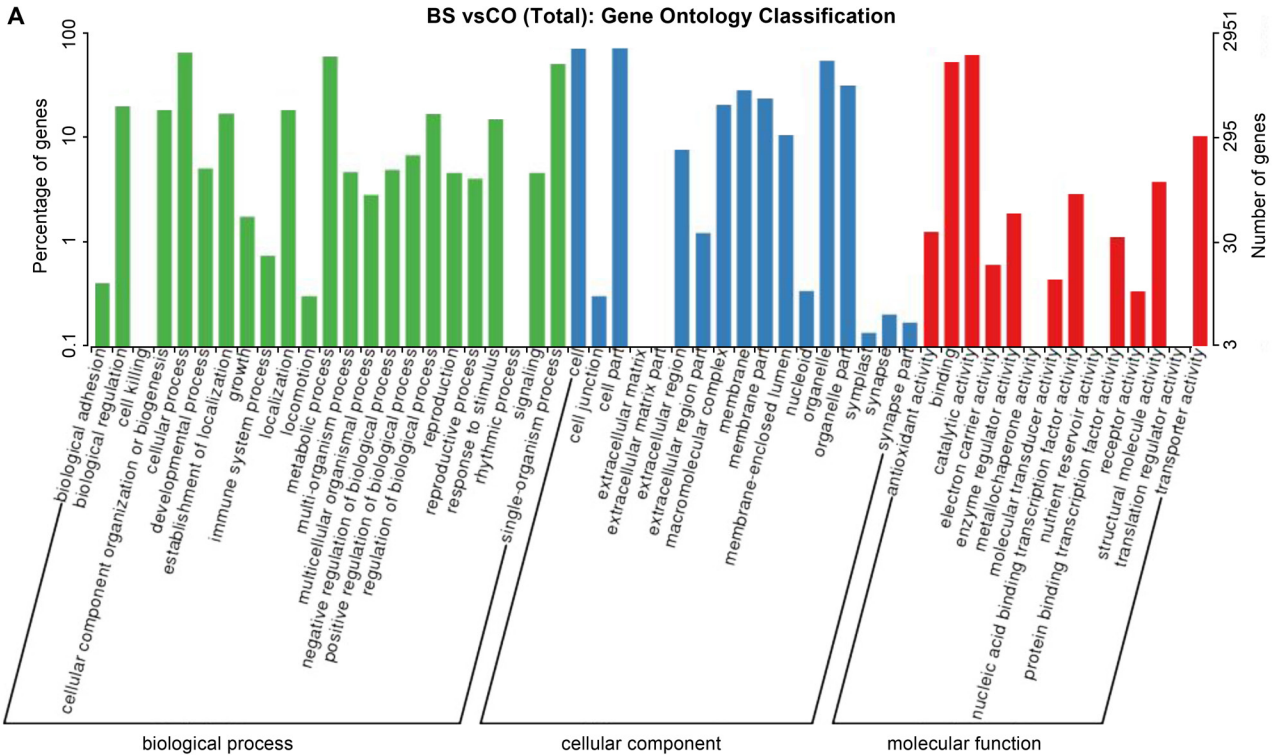


Fig. 2. Functional analysis of the DEGs.
A) Gene ontology analysis.

overview of the small RNA classification annotation results is shown in Table II.

Identification of conserved miRNAs and novel miRNAs in *M. acridum*. The known miRNAs were identified by alignment against the miRBase v. 21 data-

base. A BLAST search identified 2,350 conserved miRNAs in *M. acridum* (Table SIII). Of these conserved miRNAs, 113 were differentially expressed in BS vs. CO, including 12 upregulated miRNAs and 101 downregulated miRNAs (Fig. 3A and 3B). The length of these

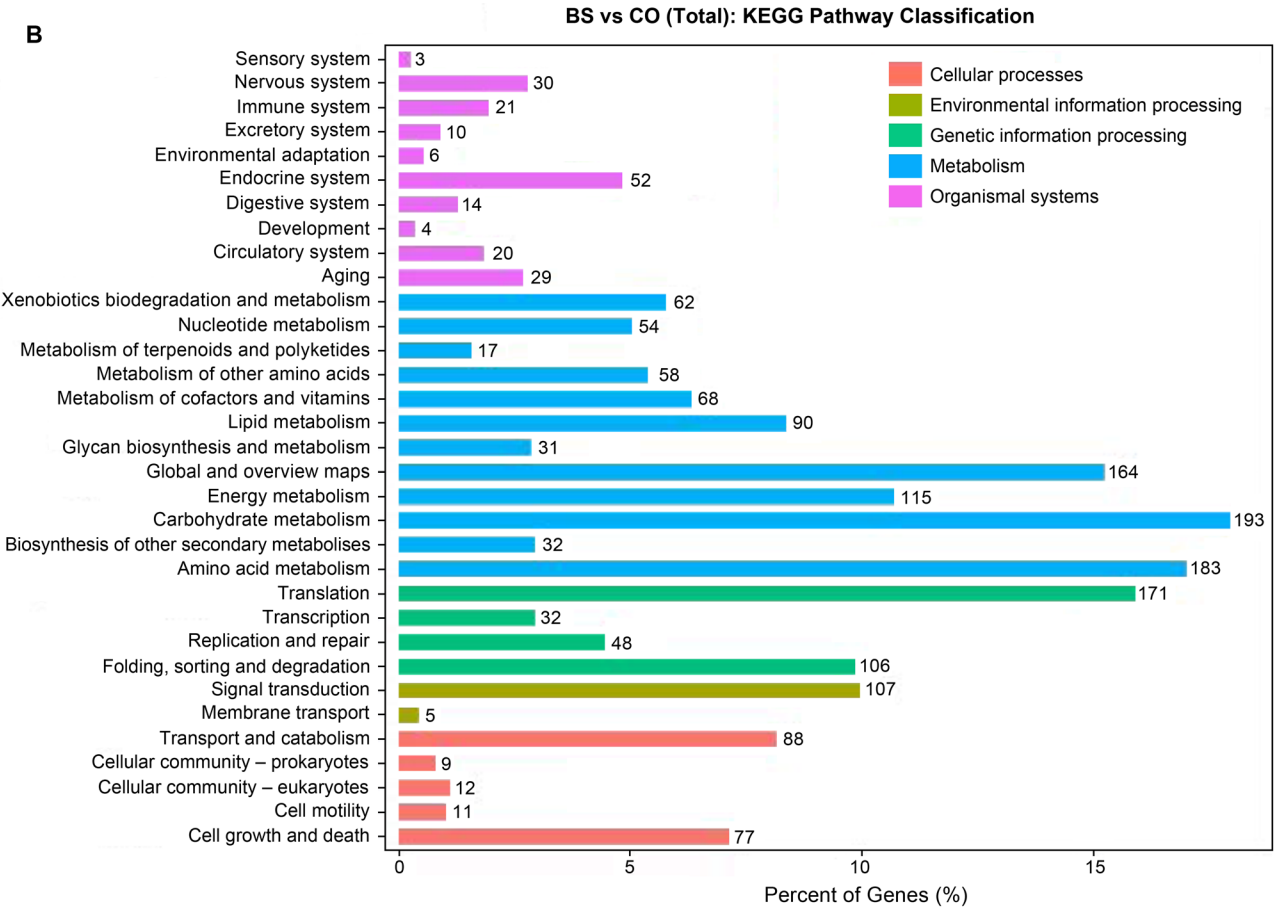


Fig. 2. Functional analysis of the DEGs.
KEGG pathway classification of DEGs in BS and CO.

milRNAs ranged from 17 nt to 25 nt and were most commonly 22 nt (Fig. 3C). They were classified into 359 conserved milRNA families, and let-7, miR-21, miR-10, miR-30 and miR-26 were the most abundant known milRNA families. The novel milRNAs were predicted by miRDeep2 software. A total of 28 novel milRNAs with lengths between 18 and 25 nt were obtained (Table SIII).

Novel 13 mature, novel 4 mature and novel 6 mature milRNAs were mostly enriched novel milRNAs.

Prediction of differential milRNA target genes and functional annotation. To understand the functions and roles of differential milRNAs target genes, the prediction of target genes was performed using the software miRanda with the following parameters: $S \geq 150$,

Table II
Summary of small RNA sequencing and annotation from BS and CO in *M. acridum*.

	BS1	BS2	BS3	CO1	CO2	CO3
Raw reads	13,988,897	11,502,145	12,788,571	14,441,950	14,456,831	14,449,135
Clean reads	11,994,110	10,092,323	10,846,886	10,825,978	12232,894	11,080,402
Mapped sRNA reads	5,691,210	4,397,198	4,929,924	5,365,353	5,761,415	5,133,510
Known milRNA numbers	828	825	765	1,441	1,479	798
Novel milRNA numbers	23	16	19	12	14	14
rRNA numbers	8,775	9,271	5,949	9,275	5,224	7,396
tRNA numbers	1,584	1,515	1,325	1,739	977	1,180
snRNA numbers	24,078	17,117	20,740	25,581	10,368	1,5410
Cis-reg numbers	6,425	3,662	4,141	6,507	5,228	4,408
Other Rfam RNA numbers	8,846	8,065	11,414	12,470	8,706	8,757
Unannotation reads	10,495,519	9,025,652	9,407,612	9096,962	11,074,942	9,625,519

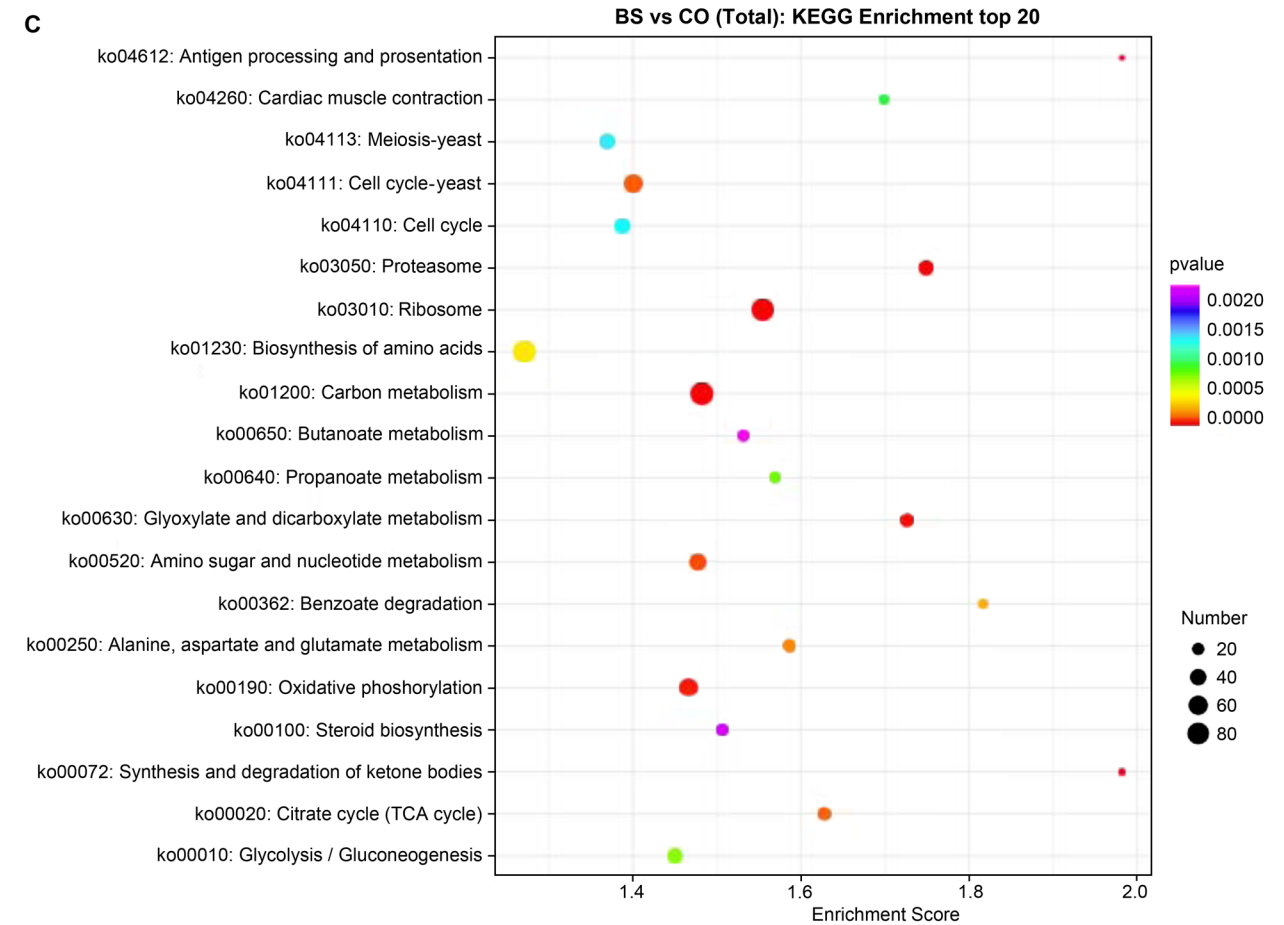


Fig. 2. Functional analysis of the DEGs.

KEGG pathway enrichment analysis of DEGs in BS and CO. The abscissa represented the enrichment score. A more significant enrichment score indicates a greater degree of enrichment. The p-value indicates the significantly enriched, and the size of the circle indicates the number of the target genes.

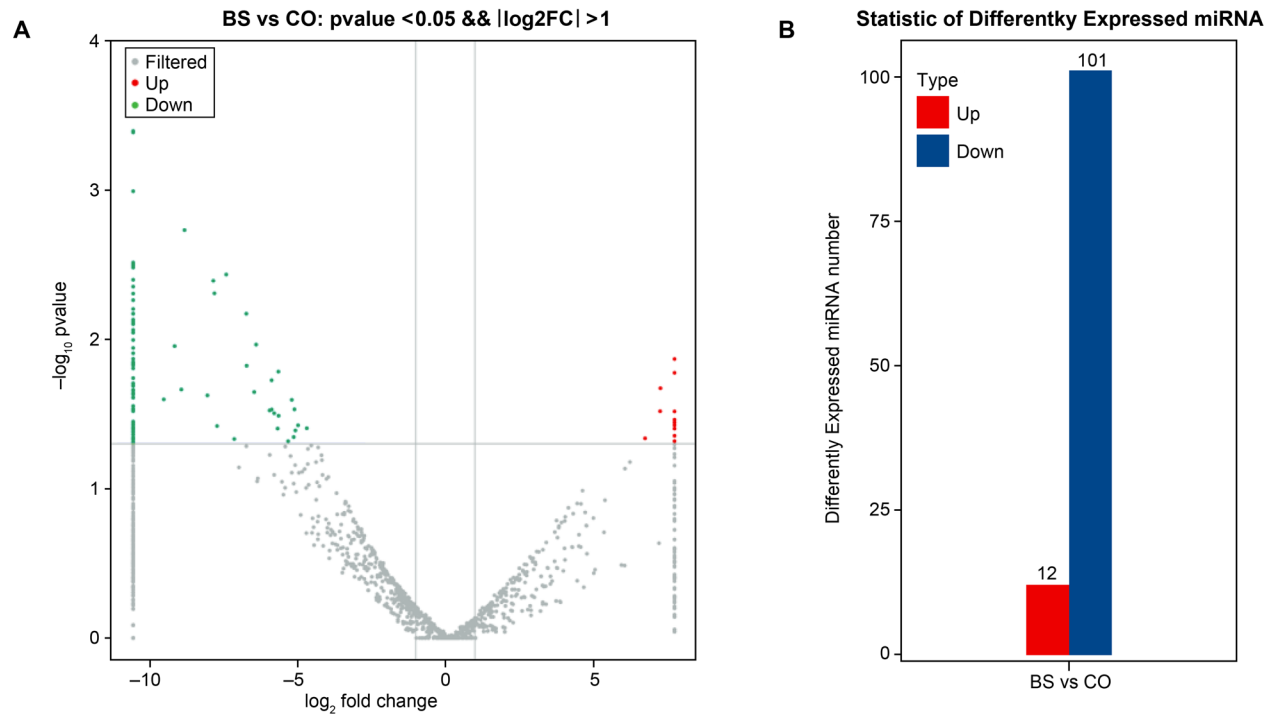


Fig. 3. Overview of the differentially expressed milRNAs (DEMs) in BS and CO. A) and B) The DEMs distribution.

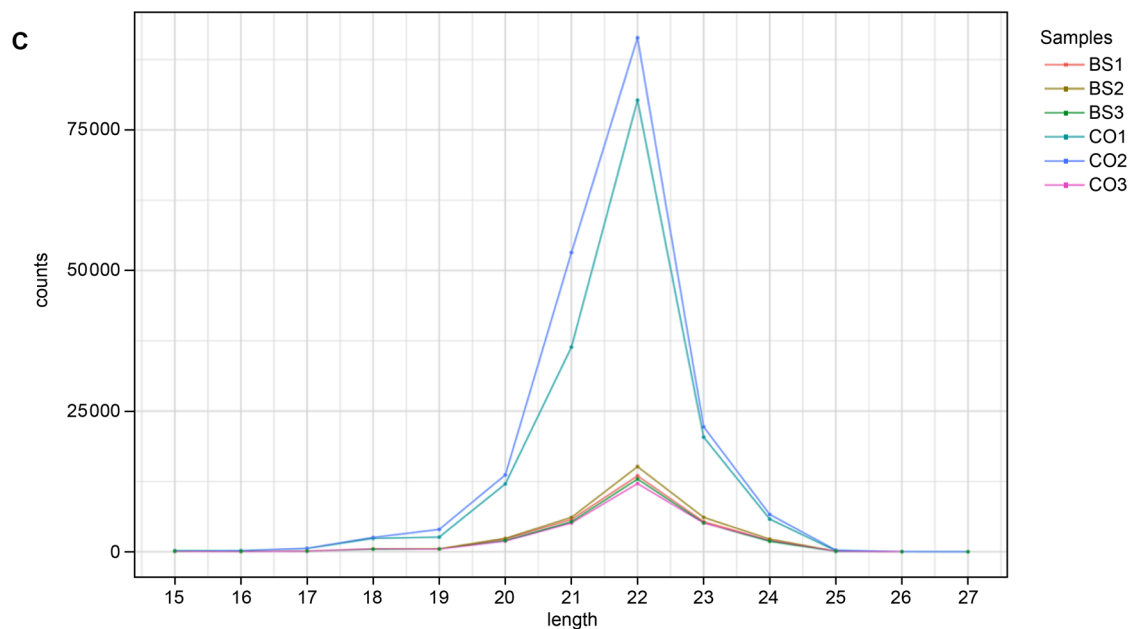


Fig. 3. Overview of the differentially expressed milRNAs (DEMs) in BS and CO.
C) The length distribution of milRNAs in six libraries.

$\Delta G \leq -30$ kcal/mol, and demand strict 5' seed pairing. In a comparison between BS and CO, 493 target genes were identified for 54 DEMs (Table SIV), whereas no targets were identified for the other 59 milRNAs. The results indicated that most milRNAs regulated more than one target gene, and different milRNAs could regulate the same target gene. Through GO enrichment

analysis, the DEMs target genes were annotated in 43 Gene Ontology (GO) terms. The GO terms with the most significant numbers of enriched target genes were cellular process (261), metabolic process (193), cell (183), cell part (183), catalytic activity (146) and organelle (133) (Fig. 4). According to Kyoto Encyclopedia of Genes and Genomes (KEGG) enrichment analysis,

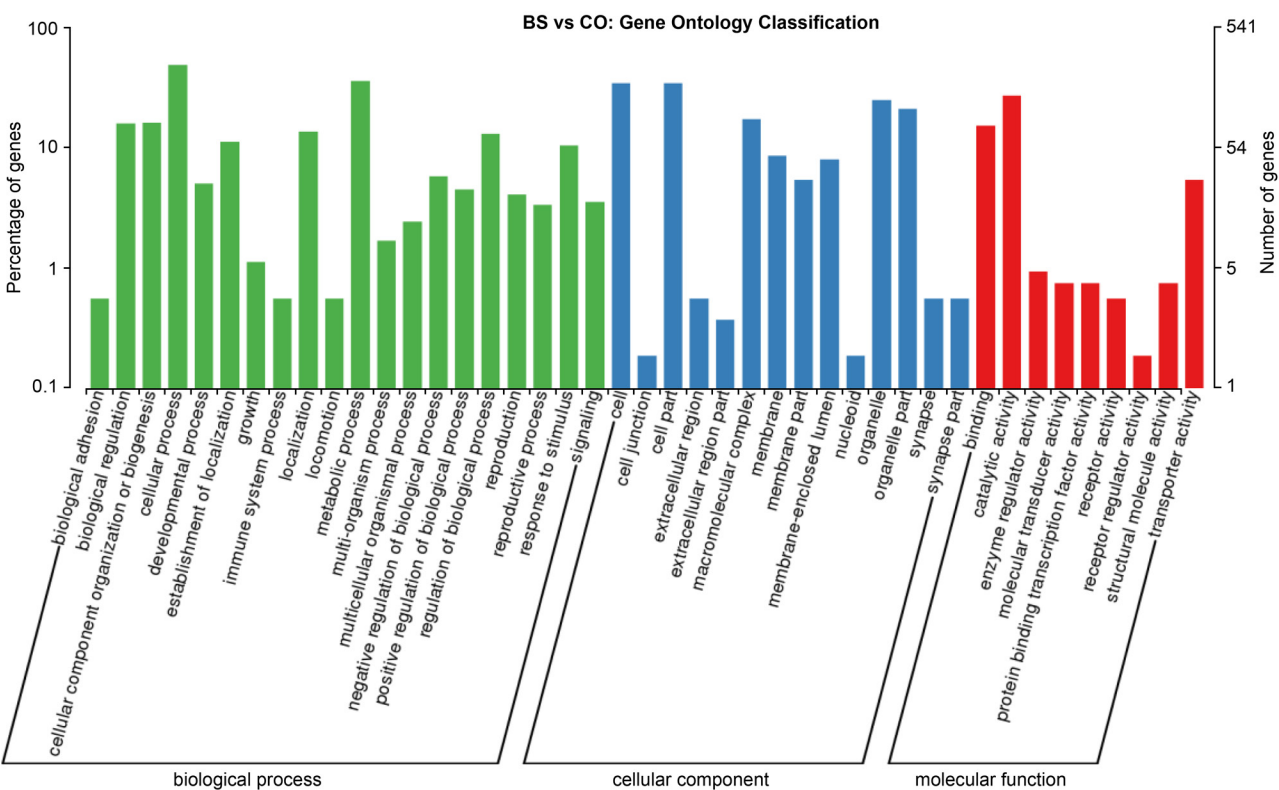


Fig. 4. GO classification analysis of the target genes of milRNAs between BS and CO in *M. acridum*.

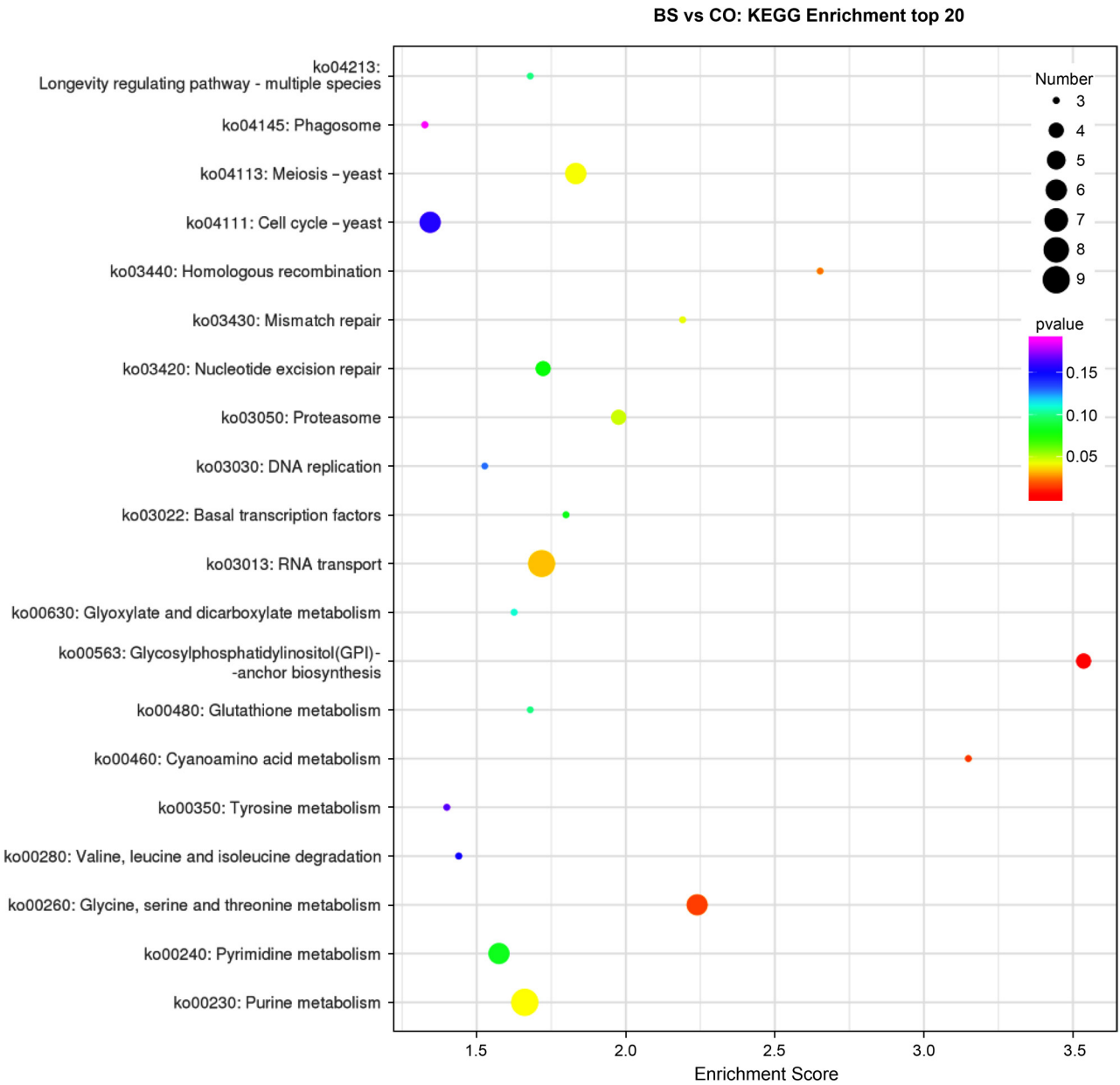


Fig. 5. KEGG enrichment analysis of the target genes of milRNAs between BS and CO in *M. acridum*. The abscissa represented the enrichment score. A more significant enrichment score indicates a greater degree of enrichment. The *p*-value indicates the significantly enriched, and the size of the circle indicates the number of the target genes.

the 20 most enriched pathways of target genes were mainly RNA transport, purine metabolism, pyrimidine metabolism, glycine, serine and threonine metabolism, and cell cycle (Fig. 5), which were the critical pathways in genetic processing, transcription, posttranscriptional regulation and metabolism.

Integration analysis of the milRNAs and mRNAs. To investigate the relationship between milRNAs and target genes, a potential milRNA-mRNA network that might affect spore morphology and structure was established. We speculated that some pathways might be associated with spore activity and characteristics, including transcriptional and posttranscriptional, cellular membrane and wall integrity, cell division, and

cellular osmotic pressure. The relationship between milRNAs and target genes is shown in Fig. 6. A total of 18 milRNAs, including two up-regulated milRNAs and 16 down-regulated milRNAs targeted 42 DEGs that included 22 up-regulated genes and 20 down-regulated genes. Of the 22 up-regulated target genes, 20 target genes corresponded to downregulated milRNAs, two target genes corresponded to two up-regulated milRNAs. The other 20 down-regulated target genes corresponded to 12 down-regulated milRNAs. Five down-regulated milRNAs corresponded to both up-regulated and down-regulated target genes. Based on these results, we conclude that several miRNA-mRNA pairs indicated negative regulation, and some

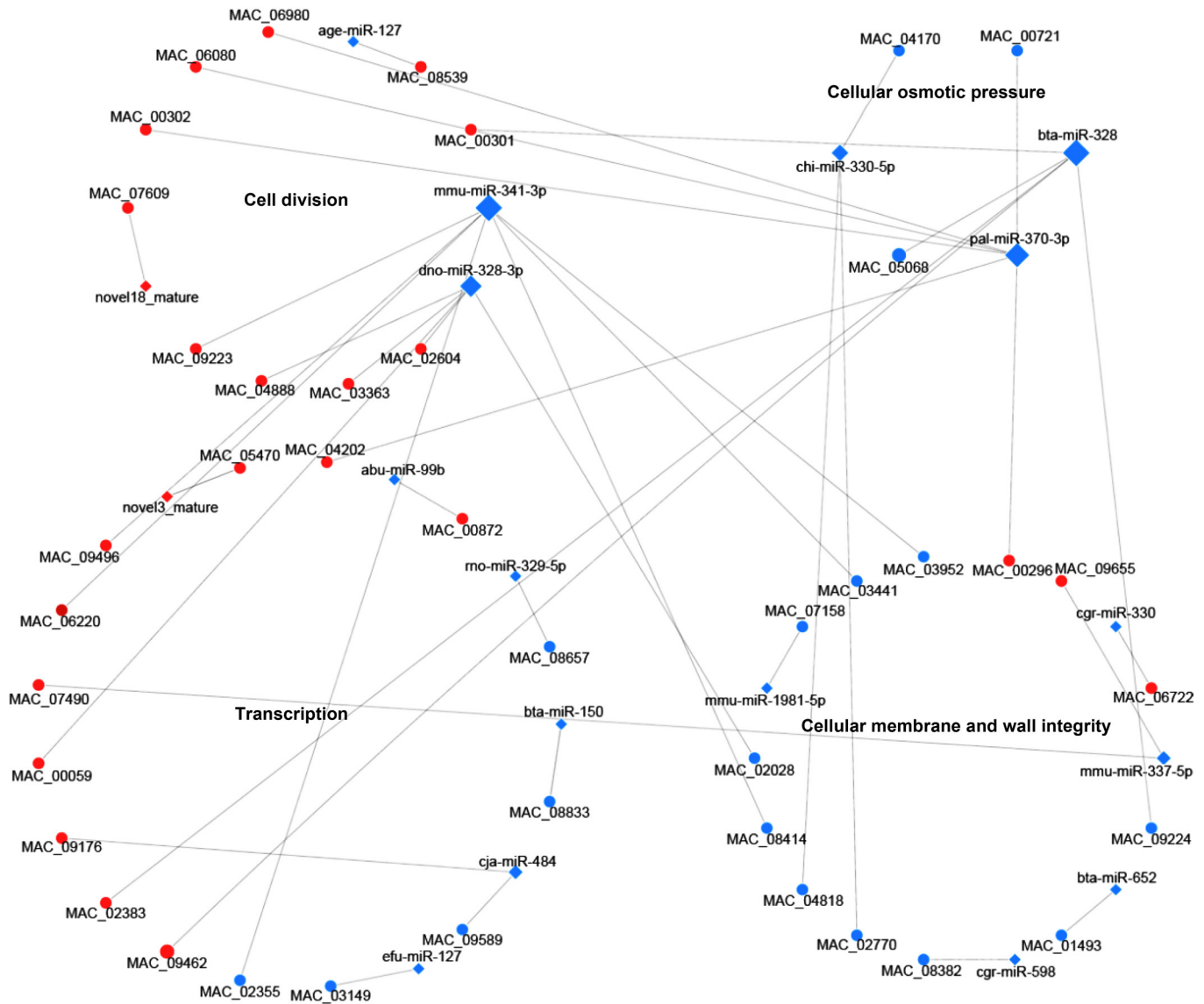


Fig. 6. The relations of the differentially expressed miRNAs and target genes. The color indicated a differentially expressed levels in BS vs. CO for miRNAs and target genes: red indicates upregulated and blue indicates downregulated.

miRNA-mRNA pairs showed the same trend in expression difference. In transcriptional and post-transcriptional, miRNAs targeted 16 DEGs, of which 10 genes were up-regulated in the BS vs CO, such as the mmu-miR-337-5p and mmu-miR-341-3p targeted MAC_07490 and MAC_06220, respectively. In a cellular membrane and wall integrity, miRNAs targeted 13 DEGs, of which 11 genes were down-regulated in the BS vs. CO, such as bta-miR-328 targeted MAC_09224, Chi-miR-330-5p targeted MAC_02770, and MAC_04818, pal-miR-370-3p targeted MAC_00296. In the cell division pathways, miRNAs targeted 10 DEGs that were significantly up-regulated, while, in cellular osmotic pressure, miRNAs targeted three DEGs that were significantly down-regulated. For all miRNA and mRNA pairs, most genes participated in transcriptional and posttranscriptional, and cell division

pathways were significantly up-regulated, while that participated in cellular membrane and wall integrity and cellular osmotic pressure were significantly down-regulated. The results indicated that miRNAs might play an important role in cell growth and cellular morphological changes.

Validation of milRNA and target gene expression with qRT-PCR. We selected six DEMs (bta-miR-150, bta-miR-328, cgr-miR-132, efu-miR-30b, efu-miR-7a, and sly-miR482c) and six DEGs (MAC_02738, MAC_03363, MAC_03964, MAC_07508, MAC_07780, and MAC_08938) to validate the accuracy of the milRNA and mRNA sequencing data using qRT-PCR. As shown in Fig. 7, all expression patterns showed similar trends. The results indicated that milRNA and mRNA sequencing data were reliable and partially validated the reliability of our findings in this study.

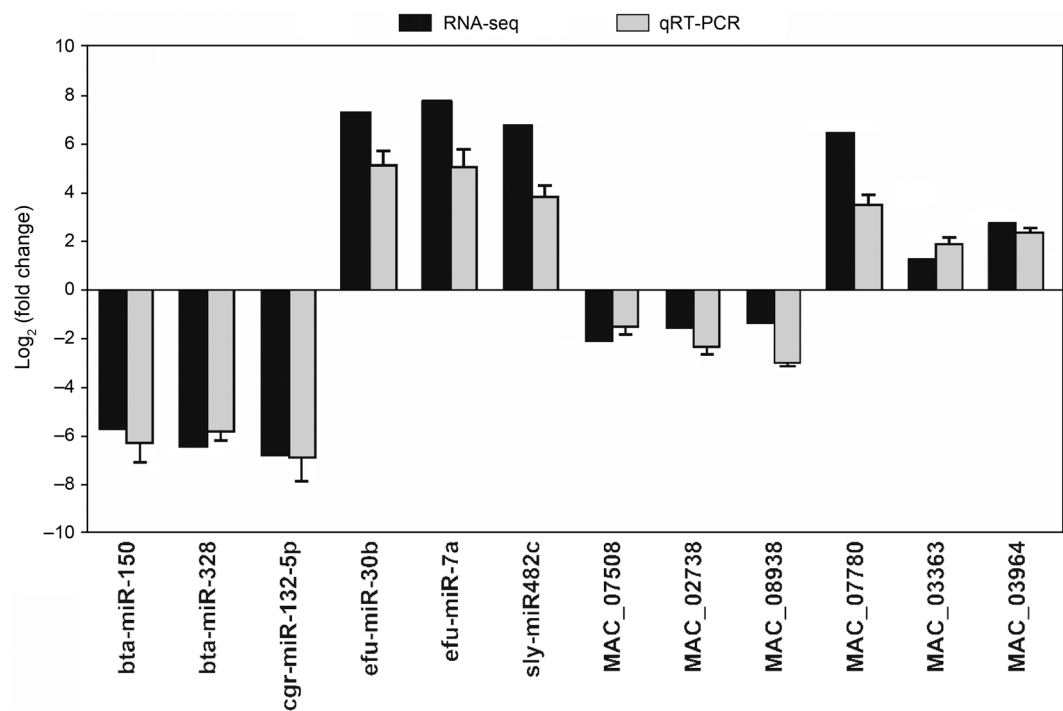


Fig. 7. Real-time PCR validation of several DEMs and DEGs.

Discussion

With people expanding their perception of the environment and health, mycoinsecticides have become increasingly important substitutes for chemical insecticides due to their low toxicity, target specificity, and harmlessness toward non-target organisms. As a microbial pesticide, *M. acridum* is widely used for locust and grasshopper control in Asia, Africa, and Australia, which is based on aerial conidia (Hunter et al. 2001; Lomer et al. 2001; Peng et al. 2008). CO and BS are two types of spores that occur in different patterns during the life cycle of *M. acridum*, and they have significant differences in cell morphology, structure, and activity. While most previous studies on the differences in BS and CO have focused on visual characteristics and field application, a few works have analyzed the molecular mechanism underlying the differences between BS and CO in fungi.

In this study, we integrated miRNA and mRNA data to identify and investigate the roles of miRNAs in spore morphological differences in the entomopathogenic fungus *M. acridum*. 4,646 DEGs were obtained between BS and CO, including 2,640 up-regulated and 2,006 down-regulated genes. GO enrichment analysis showed that the most significantly expressed genes were classified as a cellular process, metabolic process, cell, cell part, and catalytic activity. Studies have shown that BS has a thinner cell wall and lower stability and is maintained for less time than CO (Pereira and Roberts1990). The cell wall is a vital structure for fungal

cells that protect against various environmental stresses, such as heat shock, UV-B irradiation, oxidation, and desiccation. Forty cell wall glycoproteins in the filamentous fungus *Neurospora crassa* were identified by proteomic analyses, and the major cell components included chitin, β -1,3-glucan, mixed β -1,3-/ β -1,4-glucans, glycoproteins, and melanin (Patel and Free 2019). Studies have reported that *O*-mannosyltransferase and β -1,3-glucanosyltransferase mutants reduced fungal tolerance to heat shock and UV-B irradiation, formed thinner cell walls, and significantly reduced total sugar and β -1,3-glucan in entomopathogenic fungi (Luo et al. 2018; Zhao et al. 2019).

In this study, the transcriptome analysis showed that mannosyltransferase (MAC_03068, MAC_08610, MAC_05793, MAC_09434, and MAC_06369) and cell wall glucanosyltransferases Mwg1 and Mwg2 (MAC_02745 and MAC_01181) were significantly down-regulated in BS compared to CO. It might be connected to the thinner cell wall, lower stability, and shorter maintenance of BS in *M. acridum*. In *M. acridum*, β -1,3-glucan and chitin are the major polysaccharides. Synthase and hydrolytic enzymes are critical during the synthesis, branching, and cross-linking of polymers (Adams 2004). Interestingly, the expression levels of β -1,3-glucan synthase were not different between BS and CO.

In contrast, the two chitin synthases *MaChsII* and *MaChsVI* were significantly differentially expressed, down-regulated and up-regulated in BS compared to CO, respectively. Previous studies identified seven

chitin synthases in *M. acridum*, and the chitin synthase family influences *M. acridum* growth, stress tolerance, cell wall integrity, and virulence.

Regarding these two chitin synthase genes, Δ MaChsII mutants germinated more rapidly than WT, and MaChsVI participated in the chitin synthesis (Zhang et al. 2019). Chitinases and glucanases have critical roles during cell separation, cell wall modification and cell wall remodeling (Adams 2004). Seventeen and 15 differentially expressed chitinase (three down-regulated and 14 up-regulated), and glucanase (nine down- and six up-regulated) genes were identified, respectively, in this study, which might be associated with morphogenesis. KEGG pathway enrichment analysis showed that the DEGs were enriched in the biosynthesis of amino acids, carbohydrate metabolism, ribosome, and oxidative phosphorylation, resulting in a higher spore activity in BS than in CO. In addition, hydrophobin-like protein *ssgA* (MAC_07330) was significantly downregulated (\log_2 fold change = -6.36), presumably due to alterations in spore surface structures that resulted in BS hydrophilicity.

MiRNAs are a class of key regulatory factors that can partially or entirely bind to the 5'-UTR, 3'-UTR, or coding region of target genes to down- or up-regulate the expression of target genes (Grey et al. 2010; Fang and Rajewsky 2011; Reczko et al. 2012; Helwak et al. 2013; Hussain et al. 2013; Asgari, 2014). In this experiment, 2,350 conserved milRNAs were identified in the BS and CO samples of *M. acridum*. Of these conserved milRNAs, 113 milRNAs were differentially expressed in BS vs. CO, including 12 up-regulated milRNAs and 101 down-regulated milRNAs. However, only 54 DEMs, targeting 493 genes were obtained. The other 59 milRNAs were not targeted, which suggested that most fungal milRNAs were imprecisely complementary to their target genes or that the database had limitations. A similar phenomenon was also found in animals, *N. crassa* and *M. anisopliae* (Ambros 2004; Lee et al. 2010; Zhou et al. 2012).

GO classification and KEGG enrichment analyses of the target genes demonstrated that they participated in various essential genetic information processes and metabolic processes, such as translation, carbohydrate metabolism, and nucleotide metabolism, which was consistent with transcriptome analyses, indicating the potential roles of milRNA in cell morphology, structure, and activity.

Previous studies have suggested that a miRNA may not be a one-to-one target gene. A miRNA could target hundreds of genes, and an mRNA could be regulated by multiple miRNAs (O'Day and Lal et al. 2010). A similar phenomenon was found in this study; 34 DEMs were identified to have more than one target, such as bta-miR-328 targeting 65 mRNAs and mmu-miR-341-3p

targeting 83 mRNAs. Previously, miRNAs acted as negative post-transcriptional regulators that guided target gene recognition to regulate gene transcriptional start or repression (Carthew and Sontheimer 2009). Our study found that 21 DEGs (16 up-regulated and five down-regulated) displayed the opposite trend as their corresponding milRNAs at the expression level. These milRNA-mRNA pairs suggested possible negative regulation. Apart from these, 23 DEGs (22 down-regulated and one up-regulated) showed the same trend, and a similar phenomenon was found in *Trichophyton rubrum* (Wang et al. 2018). Furthermore, we found 14 milRNAs corresponding to up- and down-regulated target genes, such as down-regulated pal-miR-370-3p, which targeted 18 downregulated mRNAs and 25 upregulated mRNAs.

Previous reports have suggested that miRNAs interact with transcription factors (TFs) to regulate gene expression (Pitto et al. 2008). Our data demonstrated that five DEMs targeted six TFs in the BS vs. CO stages. For example, mmu-miR-341-3p targeted zinc finger transcription factor *ace1* and transcription factor TFIIA complex subunit *Toa1*, while pal-miR-370-3p and novel3_mature targeted HLH transcription factor and C6 transcription factor, respectively. In addition to six TFs, seven DEGs involved in transcription and transcriptional regulation were identified in the BS vs. CO stages, including RNA-directed 5'-3' RNA polymerase and eukaryotic translation initiation factor 3 subunit *EifCa*. These results indicated that milRNAs regulated gene expression at the transcription level along with TFs.

Subsequently, the milRNAs that might be involved in the control of target gene expression, related to cell morphology, structure, and activity were analyzed. Among all the DEMs, 18 associated with transcription, cell proliferation, cell wall, member integration, and cell osmotic pressure were selected. As shown in the milRNA-mRNA network, dno-miR-328-3p, novel18_mature, age-miR-127, pal-miR-370-3p and bta-miR-328 regulated eight target genes that participated in cell division and growth. In our study, dno-miR-328-3p, age-miR-127, pal-miR-370-3p and bta-miR-328 were down-regulated, and novel18_mature was up-regulated in the BS stage compared with the CO stage. For example, the dno-miR-328-3p target genes: adenosine deaminase, glycosyl hydrolase and G-patch domain protein were up-regulated. Adenosine deaminase is a well-characterized enzyme involved in the depletion of adenosine, and as an important growth factor, adenosine deaminase could participate in cell differentiation or proliferation (Maier et al. 2005; Sekiya et al. 2013).

Previous studies have suggested that glycosyl hydrolase is involved in fungal morphogenesis and bacterial cell division (Kim et al. 2002; Yakhnina and Bernhardt

2020). The age-miR-127 target gene WD repeat-containing protein pop1 was up-regulated, and WD repeat-containing protein pop1 was a component of ubiquitin-mediated proteolysis that plays a crucial role in the control of the cell cycle (Hershko 1997).

Thus, these related miRNAs might play an essential role in cell differentiation or proliferation, suggesting a probable reason of BS higher activity than CO. In addition to these miRNAs related to cell morphology, the analysis of the correlation between the expression of the miRNAs and the mRNAs showed that 11 miRNAs regulated the expression of 13 genes associated with the cell membrane and wall integrity. For example, cgr-miR-598 targeted the GPI-anchored wall transfer protein gene, which was down-regulated in the BS stage compared with the CO stage. GPI-anchored wall transfer protein is involved in cell wall construction and remodeling in *Saccharomyces cerevisiae* and likely has a role in the integration of chitin polymer within the cell wall matrix (Rodriguez-Peña et al. 2002; Kapteyn et al. 1999). The chi-miR-330-5p targeted phosphate transporter gene (*Pho88*) was also downregulated in the BS stage, and this phosphate transporter is involved in inorganic phosphate transport and mediates lipid accumulation (James and Nachiappan 2014). These results indicated that miRNAs might be involved in the cell membrane and wall integrity and play a critical role in *M. acridum*, suggesting a probably regulated function that gave BS a thinner cell wall and higher activity than conidia. Analysis of the results suggested that the miRNAs play critical roles in cell growth, cellular morphological changes, and metabolism in the entomopathogenic fungus *M. acridum*.

In summary, we first provided insight into the miRNA-mRNA relationship based on a comparison between BS and CO stages and provided useful information on the miRNAs involved in cellular morphological differences of *M. acridum*. One hundred thirteen miRNAs showed altered expression in the BS stage compared to the CO stage. The target genes of miRNAs were classified into a wide range of functional categories, especially those related to cellular processes, metabolic processes, and the cell cycle. These results suggested that miRNAs may play a critical role in cell growth, cellular morphological changes, and metabolism. The transcriptomics data also provided a foundation for further studies aimed at understanding the functions of miRNAs.

ORCID

Erhao Zhang <https://orcid.org/0000-0002-3123-8156>

Acknowledgments

The manuscript was supported by the Tibet Department of Science and Technology General Scientific Research Project (grant No. XZ2018ZRG-19). Construction of First-class Biotechnology

Major in Tibet Agricultural and Animal Husbandry University (2022-007) and Construction of Biology Teaching Experiment Platform (2022-02).

Author contributions

Conception and design of the research: E.Z. Analysis and interpretation of data: E.Z. and J.Z. Statistical analysis: R.Z., Y.L. and X.Y. Drafting the manuscript: E.Z. Revision of manuscript for important intellectual content: X.L. and Z.L. All authors have read and approved the manuscript.

Conflict of interest

The authors do not report any financial or personal connections with other persons or organizations, which might negatively affect the contents of this publication and/or claim authorship rights to this publication.

Literature

- Adámek L.** Submerge cultivation of the fungus *Metarrhizium anisopliae* (Metsch.). *Folia Microbiol* (Praha). 1965 Jul;10(4):255–257. <https://doi.org/10.1007/BF02875956>
- Adams DJ.** Fungal cell wall chitinases and glucanases. *Microbiology*. 2004 Jul 01;150(7):2029–2035. <https://doi.org/10.1099/mic.0.26980-0>
- Ambros V.** The functions of animal microRNAs. *Nature*. 2004 Sep; 431(7006):350–355. <https://doi.org/10.1038/nature02871>
- Asgari S.** Role of microRNAs in arbovirus/vector interactions. *Viruses*. 2014 Sep 23;6(9):3514–3534. <https://doi.org/10.3390/v6093514>
- Bolger AM, Lohse M, Usadel B.** Trimmomatic: a flexible trimmer for Illumina sequence data. *Bioinformatics*. 2014 Aug 01;30(15): 2114–2120. <https://doi.org/10.1093/bioinformatics/btu170>
- Bosch A, Yantorno O.** Microcycle conidiation in the entomopathogenic fungus *Beauveria bassiana* bals. (vuill.). *Process Biochem*. 1999 Sep;34(6–7):707–716. [https://doi.org/10.1016/S0032-9592\(98\)00145-9](https://doi.org/10.1016/S0032-9592(98)00145-9)
- Carthew RW, Sontheimer EJ.** Origins and mechanisms of miRNAs and siRNAs. *Cell*. 2009 Feb;136(4):642–655. <https://doi.org/10.1016/j.cell.2009.01.035>
- Fahlgren N, Carrington JC.** miRNA target prediction in plants. *Methods Mol Biol*. 2010;592:51–57. https://doi.org/10.1007/978-1-60327-005-2_4
- Fang Z, Rajewsky N.** The impact of miRNA target sites in coding sequences and in 3'UTRs. *PLoS One*. 2011 Mar 22;6(3):e18067. <https://doi.org/10.1371/journal.pone.0018067>
- Fargues J, Smits N, Vidal C, Vey A, Vega F, Mercadier G, Quimby P.** Effect of liquid culture media on morphology, growth, propagule production, and pathogenic activity of the Hyphomycete, *Metarrhizium flavoviride*. *Mycopathologia*. 2002;154(3):127–138. <https://doi.org/10.1023/A:1016068102003>
- Faria MR, Wraight SP.** Mycoinsecticides and Mycoacaricides: A comprehensive list with worldwide coverage and international classification of formulation types. *Biol Control*. 2007;43(3):237–256. <https://doi.org/10.1016/j.biocontrol.2007.08.001>
- Grey F, Tirabassi R, Meyers H, Wu G, McWeeney S, Hook L, Nelson JA.** A viral microRNA down-regulates multiple cell cycle genes through mRNA 5'UTRs. *PLoS Pathog*. 2010 Jun 24;6(6):e1000967. <https://doi.org/10.1371/journal.ppat.1000967>
- Guo JY, Wang YS, Chen T, Jiang XX, Wu P, Geng T, Pan ZH, Shang MK, Hou CX, Gao K, et al.** Functional analysis of a miRNA-like small RNA derived from *Bombyx mori* cytoplasmic polyhedrosis virus. *Insect Sci*. 2020 Jun;27(3):449–462. <https://doi.org/10.1111/1744-7917.12671>

- Guo MW, Yang P, Zhang JB, Liu G, Yuan QS, He WJ, Nian JN, Yi SY, Huang T, Liao YC. Expression of microRNA-like RNA-2 (*Fgmil-2*) and *bioH1* from a single transcript in *Fusarium graminearum* are inversely correlated to regulate biotin synthesis during vegetative growth and host infection. *Mol Plant Pathol*. 2019 Nov; 20(11):1574–1581. <https://doi.org/10.1111/mpp.12859>
- Hajek AE, McManus ML, Delalibera I. A review of introductions of pathogens and nematodes for classical biological control of insects and mites. *Biol Control*. 2007 Apr;41(1):1–13. <https://doi.org/10.1016/j.biocontrol.2006.11.003>
- Han W, Yang F, Wu Z, Guo F, Zhang J, Hai E, Shang F, Su R, Wang R, Wang Z, et al. Inner Mongolian cashmere goat secondary follicle development regulation research based on mRNA-miRNA co-analysis. *Sci Rep*. 2020 Dec;10(1):4519. <https://doi.org/10.1038/s41598-020-60351-5>
- Hegedus D, Bidochka M, Miranpuri G, Khachatourians G. A comparison of the virulence, stability and cell-wall-surface characteristics of three spore types produced by the entomopathogenic fungus *Beauveria bassiana*. *Appl Microbiol Biotechnol*. 1992 Mar; 36(6):785–789. <https://doi.org/10.1007/BF00172195>
- Helwak A, Kudla G, Dudnakova T, Tollervey D. Mapping the human miRNA interactome by CLASH reveals frequent noncanonical binding. *Cell*. 2013 Apr;153(3):654–665. <https://doi.org/10.1016/j.cell.2013.03.043>
- Hershko A. Roles of ubiquitin-mediated proteolysis in cell cycle control. *Curr Opin Cell Biol*. 1997;9(6):788–789. [https://doi.org/10.1016/S0955-0674\(97\)80079-8](https://doi.org/10.1016/S0955-0674(97)80079-8)
- Hu Z, Zhang L, Wang H, Wang Y, Tan Y, Dang L, Wang K, Sun Z, Li G, Cao X, et al. Targeted silencing of miRNA-132-3p expression rescues disuse osteopenia by promoting mesenchymal stem cell osteogenic differentiation and osteogenesis in mice. *Stem Cell Res Ther*. 2020 Dec;11(1):58. <https://doi.org/10.1186/s13287-020-1581-6>
- Hunter DM, Milner RJ, Spurgin PA. Aerial treatment of the Australian plague locust, *Chortoicetes terminifera* (Orthoptera: Acrididae) with *Metarhizium anisopliae* (Deuteromycotina: Hyphomycetes). *Bull Entomol Res*. 2001 Apr;91(2):93–99. <https://doi.org/10.1079/BER200080>
- Hussain M, Walker T, O'Neill SL, Asgari S. Blood meal induced microRNA regulates development and immune associated genes in the Dengue mosquito vector, *Aedes aegypti*. *Insect Biochem Mol Biol*. 2013 Feb;43(2):146–152. <https://doi.org/10.1016/j.ibmb.2012.11.005>
- James AW, Nachiappan V. Phosphate transporter mediated lipid accumulation in *Saccharomyces cerevisiae* under phosphate starvation conditions. *Bioresour Technol*. 2014 Jan;151:100–105. <https://doi.org/10.1016/j.biortech.2013.10.054>
- Jin Y, Zhao JH, Zhao P, Zhang T, Wang S, Guo HS. A fungal miRNA mediates epigenetic repression of a virulence gene in *Verticillium dahliae*. *Phil Trans R Soc B*. 2019;374(1767):20180309. <https://doi.org/10.1098/rstb.2018.0309>
- Kapteyn JC, Van Den Ende H, Klis FM. The contribution of cell wall proteins to the organization of the yeast cell wall. *Biochim Biophys Acta (BBA) – Gen Subj*. 1999 Jan;1426(2):373–383. [https://doi.org/10.1016/S0304-4165\(98\)00137-8](https://doi.org/10.1016/S0304-4165(98)00137-8)
- Kim D, Langmead B, Salzberg SL. HISAT: A fast spliced aligner with low memory requirements. *Nat Methods*. 2015 Apr;12(4):357–360. <https://doi.org/10.1038/nmeth.3317>
- Kim DJ, Baek JM, Uribe P, Kenerley C, Cook D. Cloning and characterization of multiple glycosyl hydrolase genes from *Trichoderma virens*. *Curr Genet*. 2002 Mar 1;40(6):374–384. <https://doi.org/10.1007/s00294-001-0267-6>
- Kumar KK, Sridhar J, Murali-Baskaran RK, Senthil-Nathan S, Kaushal P, Dara SK, Arthurs S. Microbial biopesticides for insect pest management in India: Current status and future prospects. *J Invertebr Pathol*. 2019 Jul;165:74–81. <https://doi.org/10.1016/j.jip.2018.10.008>
- Lacey LA, Frutos R, Kaya HK, Vail P. Insect pathogens as biological control agents: do they have a future? *Biol Control*. 2001 Jul; 21(3):230–248. <https://doi.org/10.1006/bcon.2001.0938>
- Lau SKP, Chow WN, Wong AYP, Yeung JMY, Bao J, Zhang N, Lok S, Woo PCY, Yuen KY. Identification of microRNA-like RNAs in mycelial and yeast phases of the thermal dimorphic fungus *Penicillium marneffei*. *PLoS Negl Trop Dis*. 2013 Aug 22;7(8):e2398. <https://doi.org/10.1371/journal.pntd.0002398>
- Lee HC, Li L, Gu W, Xue Z, Crosthwaite SK, Pertsemlidis A, Lewis ZA, Freitag M, Selker EU, Mello CC, et al. Diverse pathways generate microRNA-like RNAs and Dicer-independent small interfering RNAs in fungi. *Mol Cell*. 2010 Jun;38(6):803–814. <https://doi.org/10.1016/j.molcel.2010.04.005>
- Leland JE, Mullins DE, Vaughan LJ, Warren HL. Effects of media composition on submerged culture spores of the entomopathogenic fungus, *Metarhizium anisopliae* var. *acridum* Part 2: Effects of media osmolality on cell wall characteristics, carbohydrate concentrations, drying stability, and pathogenicity. *Biocontrol Sci Technol*. 2005 Jun;15(4):393–409. <https://doi.org/10.1080/09583150400016910>
- Li M, Xie L, Wang M, Lin Y, Zhong J, Zhang Y, Zeng J, Kong G, Xi P, Li H, et al. FoQDE2-dependent miRNA promotes *Fusarium oxysporum* f. sp. *cubense* virulence by silencing a glycosyl hydrolase coding gene expression. *PLoS Pathog*. 2022 May 5;18(5):e1010157. <https://doi.org/10.1371/journal.ppat.1010157>
- Li Y, Liu X, Yin Z, You Y, Zou Y, Liu M, He Y, Zhang H, Zheng X, Zhang Z, et al. MicroRNA-like miR236, regulated by transcription factor MoMsn2, targets histone acetyltransferase MoHat1 to play a role in appressorium formation and virulence of the rice blast fungus *Magnaporthe oryzae*. *Fungal Genet Biol*. 2020 Apr;137:103349. <https://doi.org/10.1016/j.fgb.2020.103349>
- Liu N, Tu L, Wang L, Hu H, Xu J, Zhang X. MicroRNA 157-targeted SPL genes regulate floral organ size and ovule production in cotton. *BMC Plant Biol*. 2017 Dec;17(1):7. <https://doi.org/10.1186/s12870-016-0969-z>
- Lomer CJ, Bateman RP, Johnson DL, Langewald J, Thomas M. Biological control of locusts and grasshoppers. *Annu Rev Entomol*. 2001 Jan;46(1):667–702. <https://doi.org/10.1146/annurev.ento.46.1.667>
- Luo Z, Zhang T, Liu P, Bai Y, Chen Q, Zhang Y, Keyhani NO. The *Beauveria bassiana* Gas3 β -glucanase contributes to fungal adaptation to extreme alkaline conditions. *Appl Environ Microbiol*. 2018 Aug;84(15):e01086–18. <https://doi.org/10.1128/AEM.01086-18>
- Maier SA, Galellis JR, McDermid HE. Phylogenetic analysis reveals a novel protein family closely related to adenosine deaminase. *J. Mol Evol*. 2005 Dec;61(6):776–794. <https://doi.org/10.1007/s00239-005-0046-y>
- Mukherjee K, Vilcinskis A. Development and immunity-related microRNAs of the lepidopteran model host *Galleria mellonella*. *BMC Genomics*. 2014;15(1):705. <https://doi.org/10.1186/1471-2164-15-705>
- O'Day E, Lal A. MicroRNAs and their target gene networks in breast cancer. *Breast Cancer Res*. 2010 Apr;12(2):201. <https://doi.org/10.1186/bcr2484>
- Özkan S, Mohorianu I, Xu P, Dalmay T, Coutts RHA. Profile and functional analysis of small RNAs derived from *Aspergillus fumigatus* infected with double-stranded RNA mycoviruses. *BMC Genomics*. 2017 Dec;18(1):416. <https://doi.org/10.1186/s12864-017-3773-8>
- Patel PK, Free SJ. The genetics and biochemistry of cell wall structure and synthesis in *Neurospora crassa*, a model filamentous fungus. *Front Microbiol*. 2019 Oct 10;10:2294. <https://doi.org/10.3389/fmicb.2019.02294>

- Peng G, Wang Z, Yin Y, Zeng D, Xia Y. Field trials of *Metarhizium anisopliae* var. *acridum* (Ascomycota: Hypocreales) against oriental migratory locusts, *Locusta migratoria manilensis* (Meyen) in North-eastern China. *Crop Prot.* 2008 Sep;27(9):1244–1250. <https://doi.org/10.1016/j.cropro.2008.03.007>
- Peng Y, Zhang X, Lin H, Deng S, Qin Y, Yuan Y, Feng X, Wang J, Chen, Hu F, et al. SUFU mediates EMT and Wnt/ β -catenin signaling pathway activation promoted by miRNA-324-5p in human gastric cancer. *Cell Cycle.* 2020 Oct 17;19(20):2720–2733. <https://doi.org/10.1080/15384101.2020.1826632>
- Pereira RM, Roberts DW. Dry mycelium preparations of entomopathogenic fungi, *Metarhizium anisopliae* and *Beauveria bassiana*. *J Invertebr Pathol.* 1990 Jul;56(1):39–46. [https://doi.org/10.1016/0022-2011\(90\)90142-S](https://doi.org/10.1016/0022-2011(90)90142-S)
- Pitto L, Ripoli A, Cremisi F, Rainaldi G, Rainaldi G. microRNA (interference) networks are embedded in the gene regulatory networks. *Cell Cycle.* 2008 Aug 15;7(16):2458–2461. <https://doi.org/10.4161/cc.7.16.6455>
- Reczko M, Maragkakis M, Alexiou P, Grosse I, Hatzigeorgiou AG. Functional microRNA targets in protein coding sequences. *Bioinformatics.* 2012 Mar 15;28(6):771–776. <https://doi.org/10.1093/bioinformatics/bts043>
- Rodriguez-Peña JM, Rodriguez C, Alvarez A, Nombela C, Arroyo J. Mechanisms for targeting of the *Saccharomyces cerevisiae* GPI-anchored cell wall protein Crh2p to polarised growth sites. *J Cell Sci.* 2002 Jun 15;115(12):2549–2558. <https://doi.org/10.1242/jcs.115.12.2549>
- Sekiya S, Yamada M, Shibata K, Okuhara T, Yoshida M, Inatomi S, Taguchi G, Shimosaka M. Characterization of a gene coding for a putative adenosine deaminase-related growth factor by RNA interference in the Basidiomycete *Flammulina velutipes*. *J Biosci Bioeng.* 2013 Apr;115(4):360–365. <https://doi.org/10.1016/j.jbiosc.2012.10.020>
- Shao Y, Tang J, Chen S, Wu Y, Wang K, Ma B, Zhou Q, Chen A, Wang Y. miR4 and miR16 mediated fruiting body development in the medicinal fungus *Cordyceps militaris*. *Front Microbiol.* 2019 Jan 28;10:83. <https://doi.org/10.3389/fmicb.2019.00083>
- Stephan D, Welling M, Zimmermann G. Locust control with *Metarhizium flavoviride*: New approaches in the development of a biopreparation based on blastospores. In: *New strategies in locust control*. Basel (Switzerland): Birkhäuser Verlag; 1997. p. 151–158. https://doi.org/10.1007/978-3-0348-9202-5_20
- Stief A, Altmann S, Hoffmann K, Pant BD, Scheible WR, Bäurle I. *Arabidopsis* miR156 regulates tolerance to recurring environmental stress through *SPL* transcription factors. *Plant Cell.* 2014 Apr;26(4):1792–1807. <https://doi.org/10.1105/tpc.114.123851>
- Tiño P. Basic properties and information theory of Audic-Claverie statistic for analyzing cDNA arrays. *BMC Bioinformatics.* 2009 Dec; 10(1):310. <https://doi.org/10.1186/1471-2105-10-310>
- Trapnell C, Roberts A, Goff L, Pertea G, Kim D, Kelley DR, Pimentel H, Salzberg SL, Rinn JL, Pachter L. Differential gene and transcript expression analysis of RNA-seq experiments with TopHat and Cufflinks. *Nat Protoc.* 2012 Mar;7(3):562–578. <https://doi.org/10.1038/nprot.2012.016>
- Wang L, Xu X, Yang J, Chen L, Liu B, Liu T, Jin Q. Integrated microRNA and mRNA analysis in the pathogenic filamentous fungus *Trichophyton rubrum*. *BMC Genomics.* 2018 Dec;19(1):933. <https://doi.org/10.1186/s12864-018-5316-3>
- Wassermann M, Selzer P, Steidle JLM, Mackenstedt U. Biological control of *Ixodes ricinus* larvae and nymphs with *Metarhizium anisopliae* blastospores. *Ticks Tick Borne Dis.* 2016 Jul;7(5):768–771. <https://doi.org/10.1016/j.ttbdis.2016.03.010>
- Xia Z, Wang Z, Kav NNV, Ding C, Liang Y. Characterization of microRNA-like RNAs associated with sclerotial development in *Sclerotinia sclerotiorum*. *Fungal Genet Biol.* 2020 Nov;144:103471. <https://doi.org/10.1016/j.fgb.2020.103471>
- Yakhnina AA, Bernhardt TG. The Tol-Pal system is required for peptidoglycan-cleaving enzymes to complete bacterial cell division. *Proc Natl Acad Sci USA.* 2020 Mar 24;117(12):6777–6783. <https://doi.org/10.1073/pnas.1919267117>
- Ylla G, Piulachs MD, Belles X. Comparative analysis of miRNA expression during the development of insects of different metamorphosis modes and germ-band types. *BMC Genomics.* 2017 Dec; 18(1):774. <https://doi.org/10.1186/s12864-017-4177-5>
- Zhang J, Jiang H, Du Y, Keyhani NO, Xia Y, Jin K. Members of chitin synthase family in *Metarhizium acridum* differentially affect fungal growth, stress tolerances, cell wall integrity and virulence. *PLoS Pathog.* 2019 Aug 28;15(8):e1007964. <https://doi.org/10.1371/journal.ppat.1007964>
- Zhang Z, Li T, Tang G. Identification and characterization of conserved and novel miRNAs in different development stages of *Atrijuglans heterophylla* Yang (Lepidoptera: gelechioidea). *J Asia-Pac Entomol.* 2018 Mar;21(1):9–18. <https://doi.org/10.1016/j.aspen.2017.10.014>
- Zhao T, Tian H, Xia Y, Jin K. MaPmt4, a protein O-mannosyltransferase, contributes to cell wall integrity, stress tolerance and virulence in *Metarhizium acridum*. *Curr Genet.* 2019 Aug;65(4):1025–1040. <https://doi.org/10.1007/s00294-019-00957-z>
- Zhou Q, Wang Z, Zhang J, Meng H, Huang B. Genome-wide identification and profiling of microRNA-like RNAs from *Metarhizium anisopliae* during development. *Fungal Biol.* 2012 Nov;116(11):1156–1162. <https://doi.org/10.1016/j.funbio.2012.09.001>

Supplementary materials are available on the journal's website.